

Nonlinear Chiral Meta-Mirrors: Enabling Technology for Ultrafast Switching of Light Polarization

Lei Kang,^{*,†} Cheng-Yu Wang,[†] Xuexue Guo,[†] Xingjie Ni,^{*} Zhiwen Liu,^{*} and Douglas H. Werner^{*}



Cite This: *Nano Lett.* 2020, 20, 2047–2055



Read Online

ACCESS |



Metrics & More



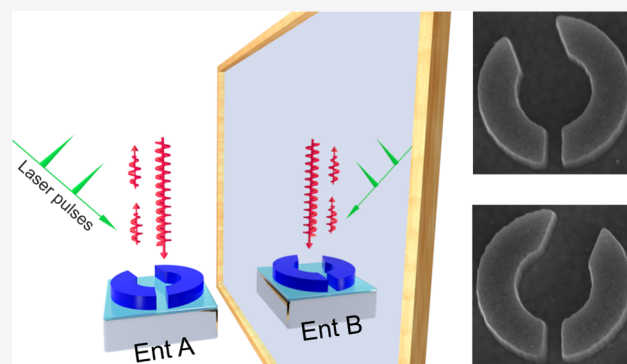
Article Recommendations



Supporting Information

ABSTRACT: Photonic nanostructures that realize ultrafast switching of light polarization are essential to advancements in the area of optical information processing. The unprecedented flexibility of metasurfaces in light manipulation makes them a promising candidate for active polarization control. However, due to the lack of optical materials exhibiting a fast as well as large refractive index change, photonic metadevices capable of ultrafast polarization switching remain elusive. Here, an ultrathin nonlinear chiral meta-mirror consisting of an array of amorphous silicon (α -Si) split-ring resonators on top of a silver backplane is demonstrated as a feasible platform for picosecond all-optical polarization switching of near-infrared light at picojoule-per-resonator pump energies. This success was made possible by the high-quality-factor resonances of the proposed meta-atoms that enable the mirror to exhibit strong chiro-

KEYWORDS: *metasurfaces, chirality, nonlinearity, optical switching, polarization*



Formed by engineered subwavelength building blocks known as meta-atoms, metamaterials have demonstrated the ability to control optical waves with unprecedented flexibility.^{1,2} As a result of the resonant nature of the meta-atoms, the greatly enhanced light–matter interaction in meta-devices affords dramatic changes in the properties of light even within a thin layer.³ In particular, controlling the polarization state of light at the subwavelength scale not only results in many intriguing phenomena but also is of fundamental importance to numerous applications in optical communication, microscopy, biochemical sensing, and so on. Importantly, chiral metamaterials demonstrate the extensive potential for polarization-sensitive nano-optical applications due to their strong chiroptical responses that surpass natural materials by many orders of magnitude. Indeed, chiral metadevices have been exploited for a variety of applications.^{4,5} As circularly polarized light (CPL) intrinsically possesses a three-dimensional (3D) structure, 3D nanoarchitectures are usually required to achieve a pronounced chiroptical response.^{6–12} However, such structures require complex nanofabrication, and more importantly, the 3D bulk structures of chiral metamaterials also render the resulting metadevices unsuitable for fast polarization switching.¹³ In particular, for ultrafast modulation based on optical excitations, bulk plasmonic nanostructures may inevitably result in poor transient response due to the undesired thermo-optical effects and the slow thermal dissipation. This limits their applications where dynamic control of light polarization is required.

and enantioselectivity. Experimental results confirm that our meta-mirrors can be used to facilitate high-speed and power-efficient polarization-state modulators.

In contrast to metamaterials that are characterized by their bulk effective optical properties, metasurfaces represent a recent advancement based on an alternative approach to manipulating the light that utilizes subwavelength-thick quasi-two-dimensional nanostructures. By engineering the structure of their meta-atoms, metasurfaces have been demonstrated to achieve complete control over the phase, amplitude, and polarization of light. The unique properties of metasurfaces have been exploited to create a number of transformative optical phenomena.^{14–19} Recently, the ability to achieve a strong chiroptical response in metasurfaces has attracted considerable attention.^{20–23} By simultaneously breaking n -fold rotational ($n > 2$) and mirror symmetries at the unit-cell level,²¹ the recently reported chiral meta-mirrors offer a unique possibility to explore strong light–matter interactions (i.e., between CPL and custom-designed metasurfaces) with just a single two-dimensional (2D) patterned layer.^{22,23} In stark contrast to conventional mirrors that flip the handedness of circularly polarized waves upon reflection, a chiral meta-mirror strongly absorbs CPL of one handedness and reflects that of the opposite handedness in a manner that preserves the

Received: January 1, 2020

Revised: February 7, 2020

Published: February 7, 2020



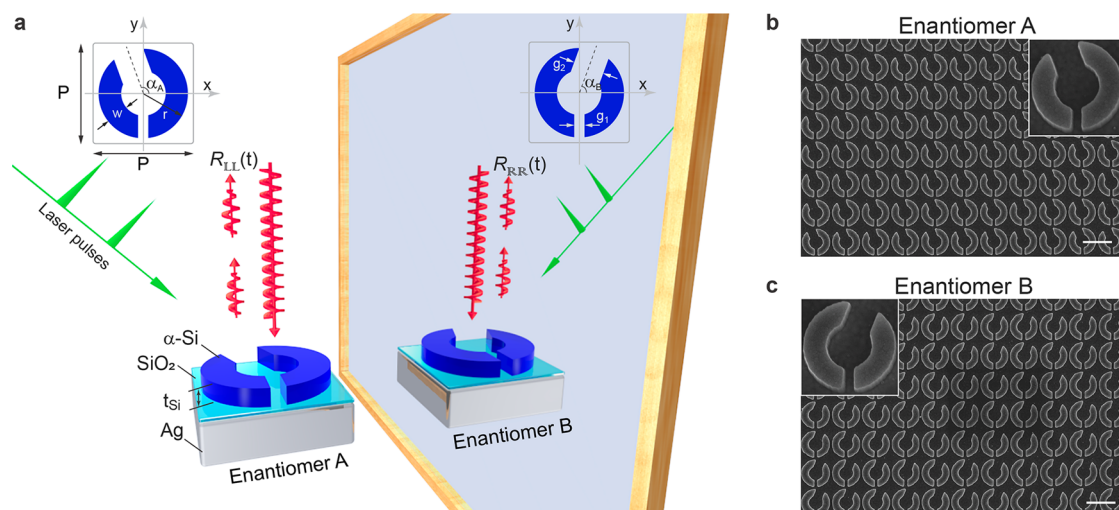


Figure 1. All-optical switching in dielectric-plasmonic hybrid chiral meta-mirrors. (a) Schematic of the enantiomeric unit cells consisting of a 2D-chiral α -Si split-ring resonator, which is separated from an optically thick silver backplane by a 30 nm thick SiO_2 spacer. The ring resonator has a broken chiral symmetry due to the unequal splits and arm lengths, which is clearly seen from the enantiomeric sketches of enantiomer A and its mirror image, i.e., enantiomer B. The silver backplane enables a handedness-selective resonant cavity, which dramatically enhances the chiroptical response of the structure. Spin- and enantioselective reflection switching of the incident circular polarizations are achieved with pulsed laser excitations, owing to the dynamics of the photoexcited carriers in the α -Si resonators. Geometrical parameters: $P = 1000$ nm, $r = 450$ nm, $w = 225$ nm, $g_1 = 100$ nm, $g_2 = 300$ nm, and $t_{\text{Si}} = 110$ nm; $\alpha_A = 180^\circ - \alpha_B = 110^\circ$. (b, c) SEM images showing enantiomers A and B of the nanofabricated chiral meta-mirrors. Enlarged SEM images for both enantiomers are also presented as insets. Scale bar represents 1 μm .

circular polarization. In these studies,^{21–23} the plasmonic nanostructures with broken 2D-chiral symmetry are responsible for the origin of chirality. Moreover, the metal/dielectric/metal sandwich structures form a spin-selective resonant cavity, leading to dramatically enhanced chiroptical responses. It is important to note that the chiral meta-mirrors allow for extraordinary chiroptical responses using rather simple planar structures, thereby significantly reducing the fabrication complexity of the corresponding metadevices.

Dielectric metasurfaces have recently been intensively studied primarily due to their capability of manipulating light with an extremely low loss. Unlike their plasmonic counterparts, dielectric metasurfaces derive their properties from electric and/or magnetic Mie resonances of high-refractive-index dielectric nanostructures even for simple shapes.^{24,25} The unique scattering characteristics of subwavelength high-index dielectric resonators can not only lead to the optical field concentration^{26–31} but they also give rise to multimodal and multipolar interference.^{25,32–34} Furthermore, the response of a dielectric material (e.g., silicon) can be more easily modulated by an external (e.g., thermal, optical, etc.) stimulus than that of a metal. However, as Mie resonances of nanostructures are primarily determined by their dielectric properties, the performance of all-dielectric metasurfaces is generally limited due to the relatively moderate values of the refractive index that are available in optical materials.^{35,36} In addition, it has been established that Mie resonances in dielectric nanostructures can be dramatically enhanced by adding a reflective backplane, which serves to facilitate interference effects in the vertical dimension.^{37,38} We have recently shown that this approach can also be exploited to facilitate low-switching-power ultrafast metadevices, which arise from high-quality (Q)-factor spectra as well as strong field confinement.³⁹ It should be noted that a highly reflective mirror has also been used to achieve an enhanced optical effect in photonic crystal slabs that support guided resonances.⁴⁰

In this work, we demonstrate all-optical picosecond light polarization switching with an ultrathin nonlinear chiral meta-mirror consisting of a 2D array of α -Si split-ring resonators on top of a silver backplane, with a thin silica spacer layer in between. The proposed meta-mirror embodies a combination of advantages of dielectric and plasmonic planar optical systems. In particular, the linear optical properties of the meta-mirror, i.e., the sharp chiral-selective absorption and the preservation of circular polarization upon reflection, are essentially attributed to two factors, the extremely low loss of α -Si at optical communication wavelengths and the Fabry–Perot interference enabled by the highly reflective plasmonic backplane. Leveraging the dynamics of the photoexcited carriers in the α -Si resonators with pump light incidence, these linear chiroptical responses can be altered dynamically, which gives rise to a strong and ultrafast polarization modulation of light in the nonlinear regime.

Figure 1a illustrates a schematic of the chiral meta-mirror's enantiomeric unit cells that consist of an α -Si split-ring resonator with broken 2D-chiral symmetry on top of an unpatterned silver backplane. This design was inspired by a previously reported chiral mirror designed to operate at microwave frequencies.⁴¹ In our design, the unequal splits and arm lengths break the 2D-chiral symmetry of the α -Si split-ring nanostructure, while the silver backplane enables the spin-dependent interference of CPL by creating an asymmetric (air/ α -Si/ SiO_2 /silver) Fabry–Perot cavity. This structure results in an enormously strong chiral-selective response to CPL. The silver backplane also ensures zero transmissivity, i.e., the absorptance satisfies $A = 1 - R$, where R represents the reflectance. A 30 nm thick SiO_2 spacer layer is introduced between the α -Si resonator layer and the silver film for optimal performance. Different from past meta-mirror embodiments based on planar plasmonic nanostructures,^{22,23} our design, which exploits the extremely low loss of α -Si at the wavelengths of interest (~ 1.5 μm), is capable of achieving a

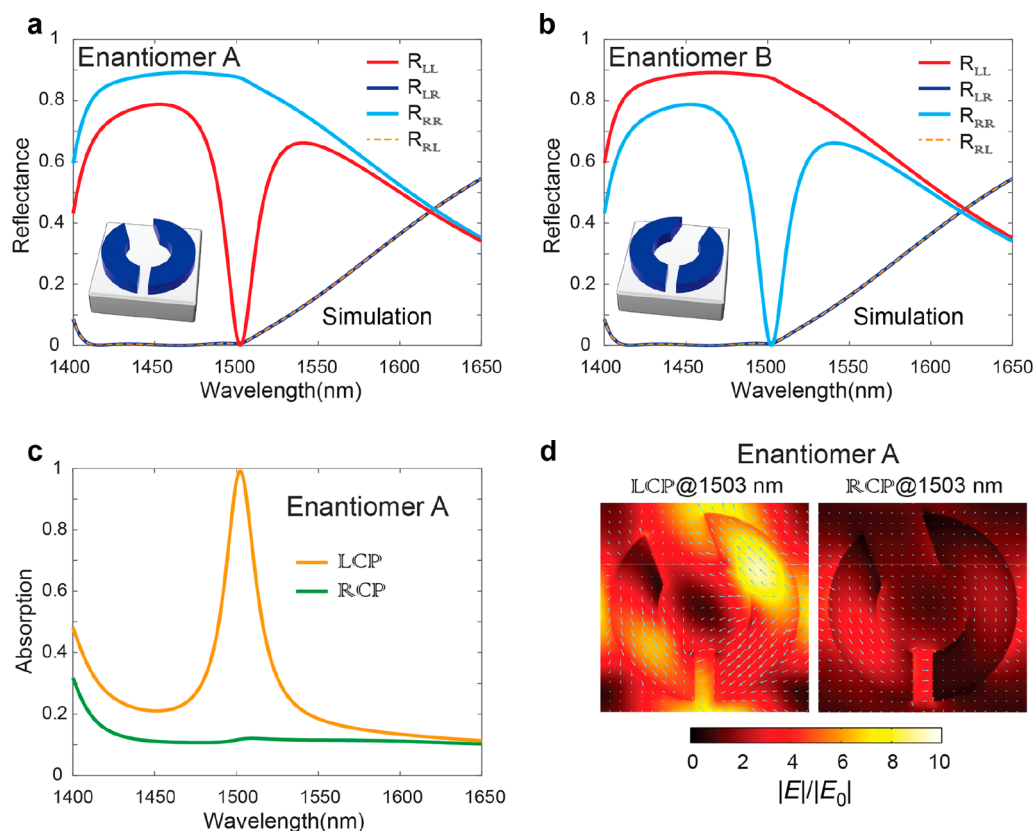


Figure 2. Simulated linear chiroptical response of both enantiomers. (a) Reflection spectra of the co- and cross-polarization components of enantiomer A under LCP and RCP illumination. (b) Reflection spectra of the co- and cross-polarization components of enantiomer B under LCP and RCP illumination. (c) The corresponding handedness-dependent total absorption spectra of enantiomer A. (d) The electric field distributions and the associated vector arrows on a plane passing through the middle of the α -Si resonator when enantiomer A is illuminated by LCP and RCP waves at a resonance wavelength of 1503 nm, respectively. The electric field magnitude is normalized to that of the incident wave.

high Q-factor chiral resonance that leads to spin-sensitive reflection (absorption) spectra.

Exploiting the carrier dynamics in α -Si under optical excitations,^{42,43} chiral meta-mirrors, therefore, can enable ultrafast optical polarization switching. As envisioned in Figure 1a, the chiral symmetry of the two α -Si resonators gives rise to the flipped spin-selectivity of the two enantiomers under the illumination of CPL. This important property affords the intrinsic enantioselectivity of the chiral meta-mirror in both the linear and nonlinear regimes. We note that our chiral meta-mirror is different from the recently reported systems for active polarization control.^{44–46} Without involving chirality, the polarization control offered by those systems is strictly valid for the case of oblique incidence. In sharp contrast, our chiral meta-mirror is designed to manipulate the polarization of light at normal incidence, which is regarded as an essential requirement for practical metadevices. Moreover, compared with the previously reported α -Si-based active metamaterials, exhibiting plasmonic resonances,^{42,43} the α -Si nanostructure in our design supports chiral resonance modes and simultaneously provides the basis for all-optical modulation. Figure 1b,c is the scanning electron microscopic (SEM) images of the fabricated samples for the two enantiomers. The total pattern size of both enantiomers was $300 \mu\text{m} \times 300 \mu\text{m}$. We emphasize that by enhancing the chiroptical response in 2D-chiral dielectric resonators; our design only requires a single nanopatterning step, which significantly reduces the fabrication complexity of the device (see Supporting Information).

To evaluate the chiroptical response of the chiral meta-mirrors, full-wave electromagnetic simulations were performed using CST Microwave Studio, a commercial finite integration package (see Supporting Information). Figure 2a shows the simulated reflectance spectra of co- and cross-polarization components of enantiomer A under left-handed circularly polarized (LCP) and right-handed circularly polarized (RCP) illumination. The power reflection coefficient R_{LL} (R_{LR}) is defined as the ratio of the power of the reflected LCP (RCP) component from the meta-mirror to that of the LCP incidence, whereas a similar meaning applies to the notation R_{RR} (R_{RL}). The fact that the power reflection coefficients of the cross-polarization components are identical, i.e., $R_{LR} = R_{RL}$, arises from the unit cell symmetry.⁵ A sharp dip is identified in the R_{LL} spectrum of enantiomer A around the resonance wavelength of 1503 nm, where, in sharp contrast, R_{RR} is greater than 0.8. The corresponding total absorption spectra are shown in Figure 2c, indicating that the chiral-selective resonance in enantiomer A leads to near unity absorption of LCP light. Results shown in Figure 2a,c unambiguously reveal the two distinctive characteristics of the chiral meta-mirror, i.e., the ability to preserve polarization upon reflection and the spin-dependent absorption. As expected, Figure 2b shows that enantiomer B exhibits a handedness-flipped chiroptical response when illuminated by CPL, further suggesting the enantiomeric characteristic of the structure. It should be noted that, distinct from the chirality found in plasmonic nanostructures,^{22,23} the observed extraordinary chiroptical

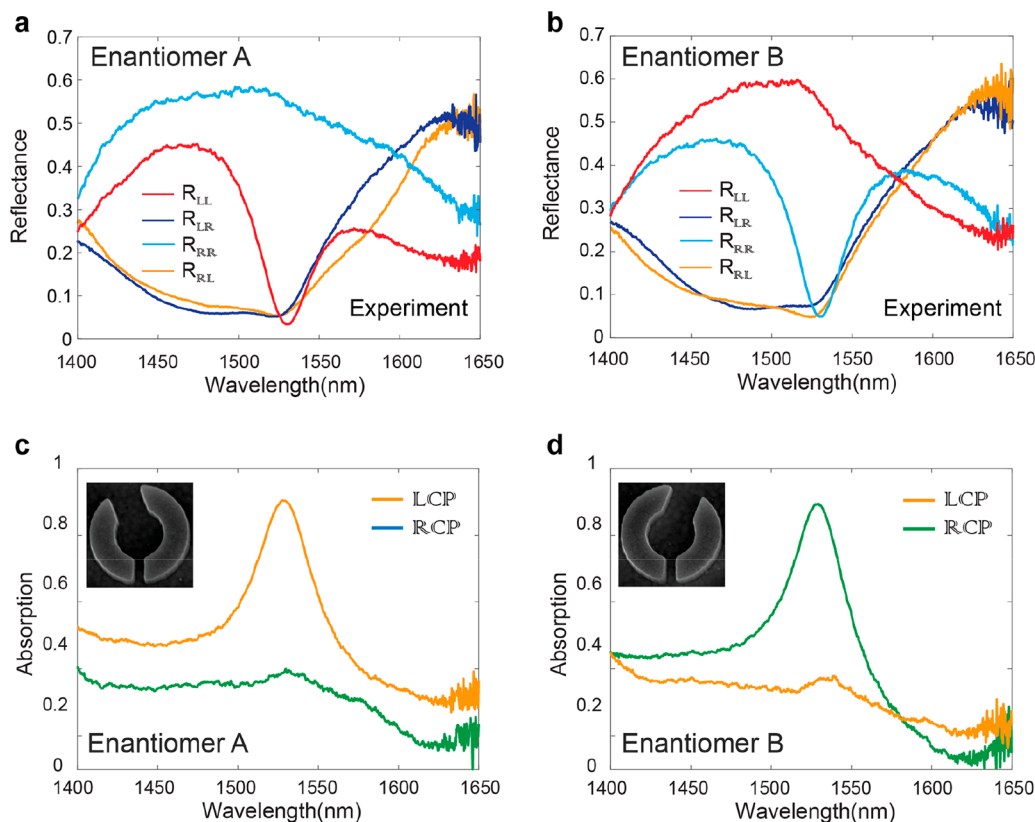


Figure 3. Measured linear chiral response of both enantiomers. (a, b) Measured reflection spectra of the co- and cross-polarization components of enantiomer A and enantiomer B. (c, d) The corresponding handedness-dependent total absorption spectra of enantiomer A and enantiomer B.

responses arise from the Mie resonance of the α -Si split rings. As shown in Figure 2d, this is made evident from the simulated electric field distribution on a plane passing through the middle of the dielectric resonator. In particular, the spin-dependent local field enhancement arising from the chiral-selective resonance of enantiomer A results in the distinct absorption in the silver backplane at the resonant wavelength. We note that the chiroptical response of the proposed meta-mirrors is directly determined by the symmetry property of the unit cell; for a systematic study, refer to Figure S2 in the Supporting Information. In addition, in the absence of a backplane, the array of 2D-chiral α -Si resonators exhibits no chiroptical response in the far-field (Figure S3 in Supporting Information).

In order to characterize the chiroptical responses of the meta-mirrors, we illuminated the fabricated samples of both enantiomers with circularly polarized waves and obtained reflection coefficients by using a microspectroscopy setup (see Supporting Information). The measured reflectance results are shown in Figure 3a,b, where all spectra were normalized to that of a bare silver substrate. A sharp dip can be identified in the R_{LL} spectrum of enantiomer A at wavelengths around 1530 nm, while the corresponding R_{RR} spectrum exhibits a high reflectivity (>0.5) in the same wavelength band. The corresponding spin-dependent total absorption spectra of enantiomer A are shown in Figure 3c. In comparison, as illustrated in Figure 3b,d, enantiomer B exhibits a complementary chiral reflection behavior. In brief, the fabricated chiral meta-mirrors strongly absorb CPL of one handedness and preserve the polarization state of the other upon reflection. The measured results are in good agreement with the

simulation data shown in Figure 2, with slight discrepancies likely arising from fabrication imperfections. We note that the spectra shown in Figure 3 reveal that our chiral meta-mirrors yield a narrow-band chiral resonance, which is explicitly distinct from the plasmonic chiral metamaterials reported previously.^{9,10} In particular, the measured R_{LL} spectrum of enantiomer A and the R_{RR} spectrum of enantiomer B reveal a Q-factor (defined as $\lambda/\Delta\lambda$) of ~ 56 and ~ 46 , respectively. This is comparable to what has been observed in mid-infrared chiral metasurfaces composed of high-aspect-ratio asymmetric Si resonator arrays, which are capable of supporting Fano resonances.²⁰

Unlike the meta-atoms (such as the gold helices⁶) in which the circular polarization states correspond to the eigenmode resonance of the structure, the chiroptical response observed here originates from both the intrinsic chiral property of the proposed meta-mirror and its optical anisotropy. The latter, stemming from the lack of in-plane rotational symmetry of the unit cell, leads to the polarization-dependent optical response to a linearly polarized wave. To provide a complete picture of the reflection behavior of our chiral meta-mirrors, the samples of both enantiomers were illuminated by a linearly polarized wave at a series of azimuthal angles φ , and the polarization ellipse of the reflected waves was then characterized (see Supporting Information). The measured ellipticity (η) and polarization rotation angle (θ) are summarized in Figure 4a–d, while the simulated power loss density (PLD) distribution on the surface of the silver backplane for several values of φ is presented in Figure 4e. The corresponding discussion is provided in the Supporting Information.

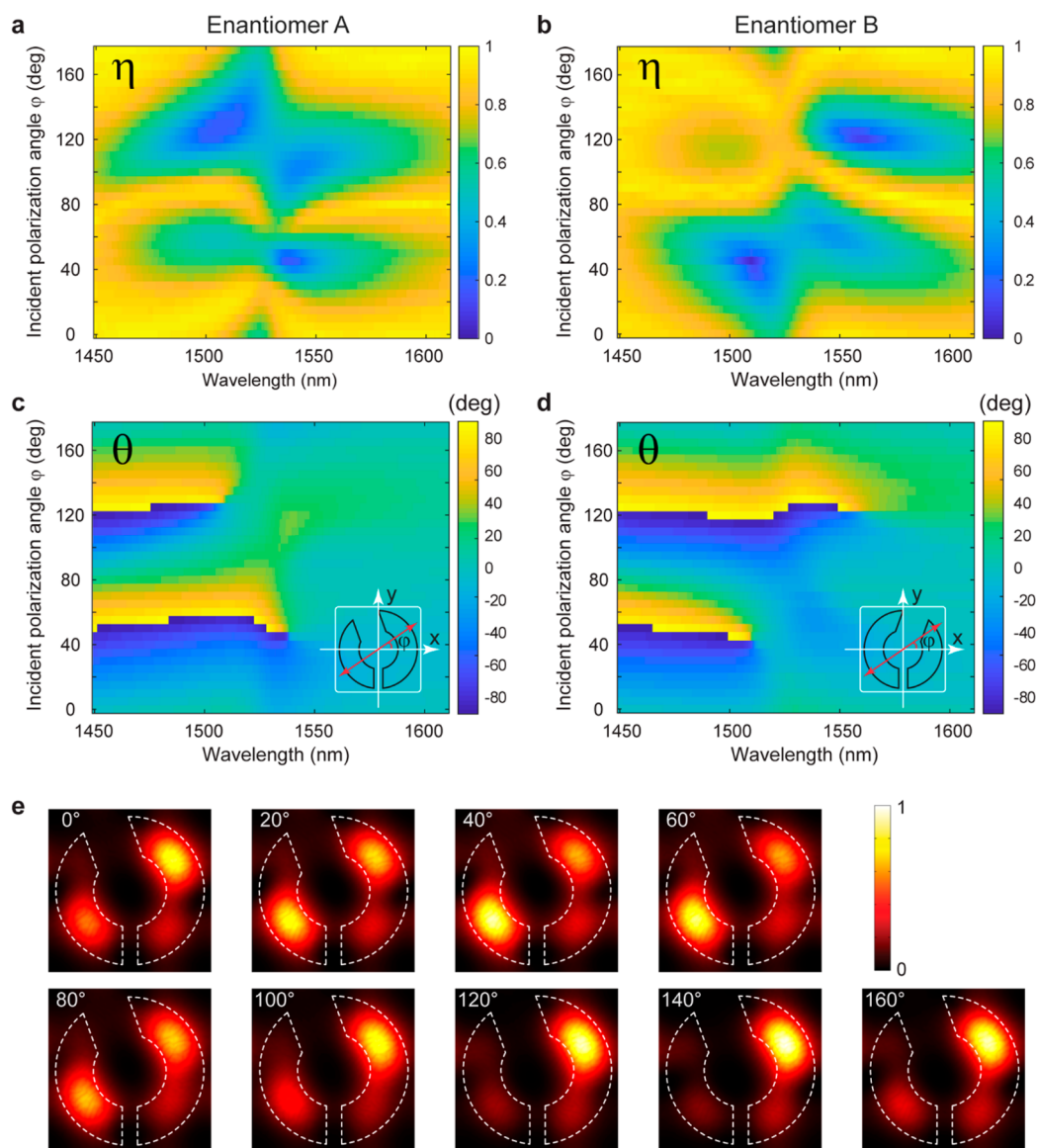


Figure 4. Experimental characterization of the polarization state upon reflection. (a, c) Ellipticity (η) and polarization rotation angle (θ) as a function of the wavelength and azimuthal angle (φ) of the linearly polarized incident light impinging upon enantiomer A. (b, d) η and θ as a function of the wavelength and azimuthal angle (φ) of the linearly polarized incident light impinging upon enantiomer B. (e) Evolution of the simulated PLD distribution on the surface of the silver backplane (enantiomer A) at the resonance wavelength of 1503 nm as a function of φ .

The ultrafast modulation of the chiral meta-mirror was studied using a pump pulse to photoexcite carriers in the α -Si, and a near-infrared probe pulse was utilized to characterize the time-dependent change in the chiral-selective reflection. More details of the pump-probe measurements can be found in the [Supporting Information](#). Since the pump beam size (~ 3 mm in diameter) was much larger than the samples' footprint, it can be assumed that the corresponding photoexcitation is uniform, and the maximal pumping power is ~ 4.0 pJ-per-resonator. Considering the symmetry in the enantiomeric response of the two enantiomers, the remaining pump-probe studies were carried out using enantiomer A. Moreover, given the extremely low cross-polarized reflection behavior, only pump-induced changes in the copolarized reflection ($R_{\parallel\parallel}$ and $R_{\parallel R}$) were measured.

Figure 5 illustrates the chiral-selective reflection modulation of enantiomer A at a series of wavelengths around the resonance resulting from pump-probe experiments using a

pump intensity (I_p , in terms of peak power density) of 0.07 GW cm^{-2} . For $R_{\parallel\parallel}$, a peak switching ratio ($\Delta R_{\parallel\parallel}/R_{\parallel\parallel}$) of more than 60% is observed for a zero pump-probe delay time (i.e., $\Delta t = 0$) at the resonance wavelength of 1530 nm. As the probe wavelength is moved from the shorter- to the longer-wavelength side of the resonance, the peak switching ratio of $R_{\parallel\parallel}$ exhibits a sign flipping. A fast (~ 10 ps) component and a slow nanosecond component are observed in most of the traces shown in Figure 5a, which agrees with the transient response observed in previously reported α -Si-based active metamaterials.^{42,43} It should be noted that, considering the time-bandwidth product (TBP), which determines the correlation between the pulse duration ($\Delta\tau$) and bandwidth ($\Delta\lambda$), pump pulses with a finite duration of ~ 1 ps ($\Delta\lambda \sim 1$ nm) are used to resolve the high Q-factor resonances observed in our chiral meta-mirrors. Compared with the femtosecond (fs) pump pulses used in previous work,^{42,43} the ps pump pulses employed in our study resulted in a ~ 3 ps rise time,

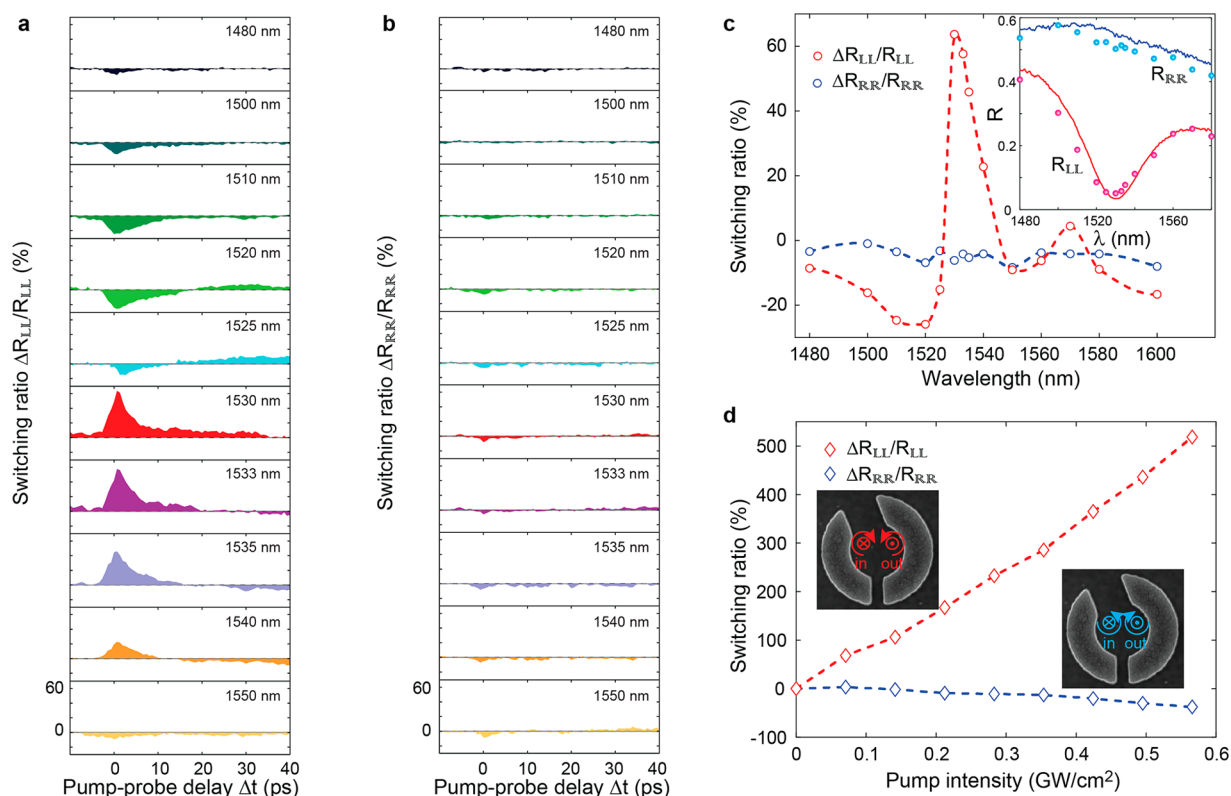


Figure 5. Pump–probe spectroscopy of chiral-selective reflection dynamics. (a) Comparison of the pump–probe signal associated with R_{LL} modulation for a series of probe wavelengths around the resonance of enantiomer A. (b) The corresponding pump–probe signal for R_{RR} modulation. The chiral meta-mirror is excited by pump pulses of constant intensity (I_{pump}) of 0.07 GW cm⁻². (c) Switching ratio spectra, resulting from the pump–probe spectroscopy. The empty circles represent the measured data obtained by integrating the pump–probe signal peaks found in panels a and b, and the dashed curves represent interpolated data. Inset: The corresponding reflectance spectra with (markers) and without a pump (curves). (d) Pump power dependences of the maximum switching ratio at a probe wavelength of 1530 nm. Inset: Schematic of the spin state of the probe pulses in the corresponding measurements.

corresponding to the width of the pump–probe cross-correlation. This suggests that a steeper rising edge may be achieved by pumping the chiral meta-mirror with short-duration pulses, however, with a trade-off in wavelength resolution. Furthermore, the traces in Figure 5a also reveal a long-lasting component ($\Delta t \sim 20\text{--}40$ ps) in $\Delta R_{LL}/R_{LL}$ at some probe wavelengths (e.g., 1525 and 1540 nm). This observation can be attributed to the competition between the free-carrier relaxation process in α -Si and the slow thermal effect due to lattice heating.⁴⁷ In sharp contrast, no significant modulation was observed in the pump–probe signal of $\Delta R_{RR}/R_{RR}$ (Figure 5b).

In order to better elucidate the correlation between the resonance behavior of the ultrafast modulation and the corresponding linear chiral response, in Figure 5c, we present the switching ratio spectra, which are generated by integrating the pump–probe signal peaks found in Figure 5a,b. Evidently, the pump–probe signal is closely dependent on the spin of the probe light and the chiral-selective resonance of enantiomer A in the linear regime. The inset of Figure 5c depicts the corresponding reflectance spectra of the photoexcited chiral meta-mirror at $\Delta t = 0$ and those without a pump, in which the pump-induced spectral changes of R_{LL} and R_{RR} around the resonance were clearly identified. We note that, although the absolute reflectance change in ΔR_{RR} is comparable to that found in ΔR_{LL} , the LCP linear response of enantiomer A (Figure 3a) enables the remarkable LCP reflection switching

around the resonance. On the other hand, the observed simultaneous modulation of both circular polarizations indicates the potential of our meta-mirrors for ultrafast polarization-state control.

The characterization of pump power dependence of the meta-mirror's switching behavior is of significant practical importance for the development of corresponding metadevices. To this end, we performed pump–probe experiments with increasing pump power I_p at a fixed probe wavelength of 1530 nm, where the corresponding maximal switching ratio is shown in Figure 5d. A strong chiral selectivity is identified: the on-resonance maximal $\Delta R_{LL}/R_{LL}$ reaches an extraordinary value of $\sim 518\%$ when I_p was increased to 0.57 GW cm⁻² and, in contrast, $\Delta R_{RR}/R_{RR}$ approaches $\sim -37\%$. Within the pump power range studied, no saturation was observed. We emphasize that, using a similar pumping intensity, a transmission modulation of $\sim 1\%$ was recently observed in an all-dielectric metasurface consisting of an array of α -Si nanodisks.³⁶ In addition, the maximal pump intensity in our experiments was more than 1 order of magnitude lower than that used in the recent demonstration of switchable nonlinear metamaterials based on gold nanorods.⁴⁵ Moreover, the linear power dependence of the switching ratio identified in Figure 5d would be beneficial in applications where modulation-level control is required.

The observed chiral-selective nonlinear dynamics essentially confirm the potential of these meta-mirrors for achieving

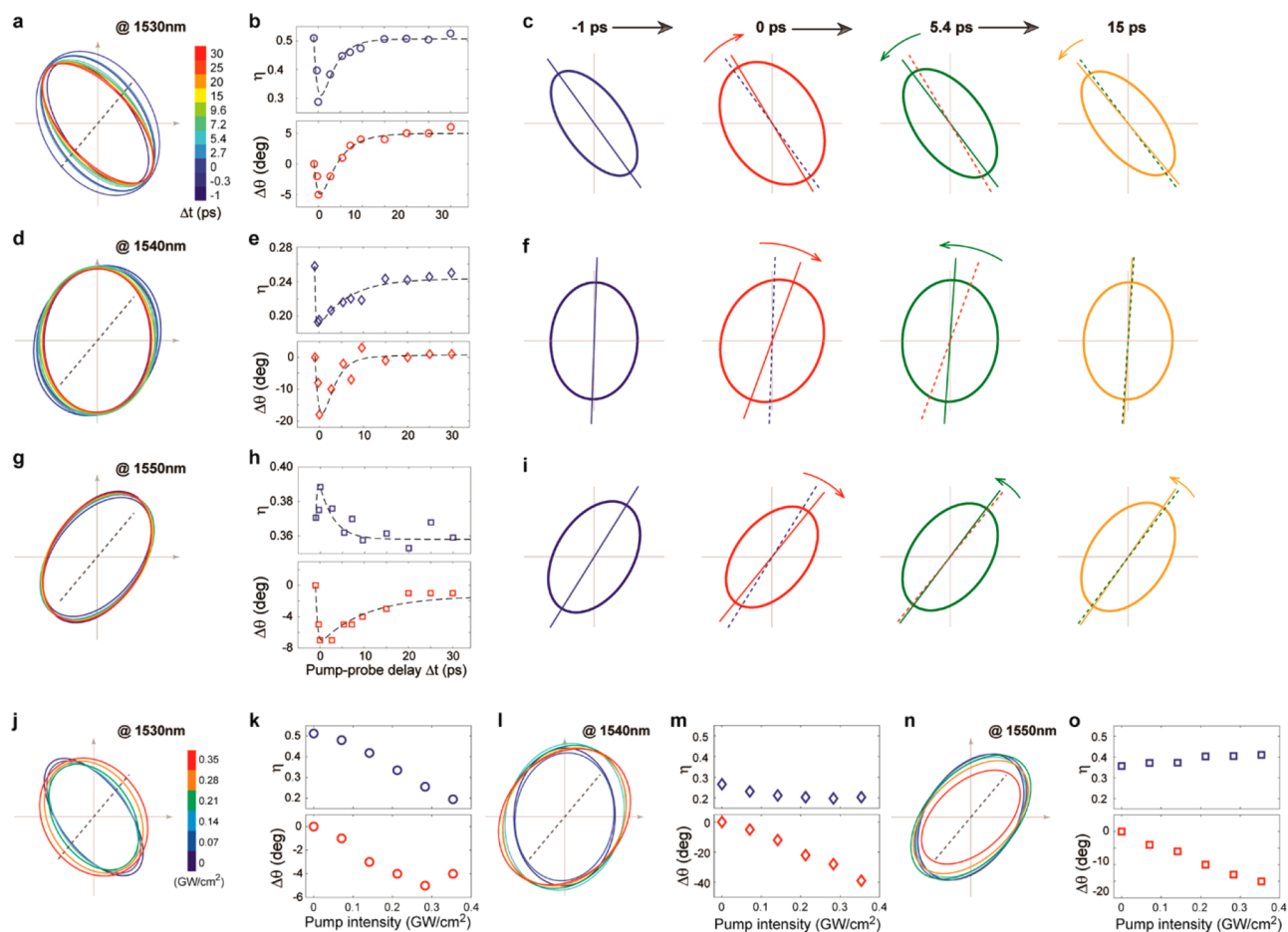


Figure 6. Picosecond optical switching of light polarization. (a) The polarization ellipses of the reflected wave at 1530 nm for a series of probe–pump time delays (Δt). The gray dashed line indicates the incident light polarization. (b) The corresponding pump-induced ellipticity (η) and polarization angle modulation ($\Delta\theta$) versus Δt . The dashed line in both panels represents a triple exponential fit to the measured data (open markers). (c) The corresponding evolution of the polarization ellipse at $\Delta t = -1, 0, 5.4,$ and 15 ps. $\Delta t = -1$ ps is referred to as the static state. The dashed line in each panel represents the orientation direction of the previous polarization ellipse. (d–f) Same as panels a–c, but for the reflected wave at 1540 nm. (g–i) Same as panels a–c, but for the reflected wave at 1550 nm. For the results shown in panels a–i, a pump intensity of $I_p = 0.20 \text{ GW cm}^{-2}$ was used. (j–o) Intensity-dependent polarization state switching. (j) The polarization ellipses of the reflected wave at 1530 nm for a series of pump intensities, I_p . The gray dashed line indicates the incident light polarization. (k) The corresponding pump-induced ellipticity (η) and polarization angle modulation ($\Delta\theta$) versus I_p . (l–m) Same as panels j and k, but for the reflected wave at 1540 nm. (n–o) Same as panels j and k, but for the reflected wave at 1550 nm.

ultrafast switching of polarized light. To characterize the polarization switching effect, pump–probe measurements were carried out using an experimental setup with a polarization-analyzing unit included. In particular, a linearly polarized probe pulse and an 800 nm pump pulse were used to measure the time-resolved polarization ellipse of the reflected wave from enantiomer A (see Supporting Information). To highlight the flexibility offered by the proposed meta-mirror in light polarization synthesis, but without loss of generality, we fixed the incident polarization angle φ to 50° .

Figure 6a–i conveys the measured dynamics of the reflected polarization state at the wavelengths of 1530, 1540, and 1550 nm. A series of pump–probe experiments were performed, where the resulting polarization ellipses corresponding to the reflected wave at 1530 nm for a series of Δt are shown in Figure 6a. By evaluating these polarization ellipses, as shown in Figure 6b, we further obtained the corresponding time-dependent modulation of ellipticity (η) and polarization angle ($\Delta\theta = \theta_{\Delta t} - \theta_{\text{static}}$, where $\theta_{\Delta t}$ and θ_{static} are the orientation angles associated with the polarization ellipse of the

reflected wave at Δt and in the static state, respectively). A component with a very rapid rise time ~ 1 ps was identified in both traces, which has a concomitant ~ 0.2 and $\sim 5^\circ$ change in η and $\Delta\theta$ at zero pump–probe delays ($\Delta t = 0$), followed by a slower ~ 10 ps recovery process. The observed sign flipping and the long-duration plateau in the $\Delta\theta$ trace (lower panel of Figure 6b) arise from the competition between the free-carrier relaxation and lattice heating processes in $\alpha\text{-Si}$.⁴⁷ The evolution of the polarization ellipse in Figure 6c more clearly shows the pump-induced dynamic modulation of the polarization state. Furthermore, for the wavelength of 1540 nm (Figure 6d–f), a maximum $\Delta\theta$ modulation as large as 20° was observed at $\Delta t = 0$, accompanied by a relatively small change in η . Along with the results at a 1550 nm wavelength (Figure 6g–i), Figure 6a–i reveals the optical excitation enabled strong modulation of the polarization states of reflected light within the resonance band of enantiomer A. The strong wavelength-dependence seen in Figure 6a–i is consistent with the sharp resonance identified in the linear chiroptical response of the meta-mirror.

Given that the refractive index change of α -Si and subsequently the resonance shift of the chiral meta-mirror varies with the optical excitation intensity, the polarization state of a reflected wave can be controlled by varying the pump intensity, I_p . Consequently, by varying I_p and collecting the pump–probe signal at $\Delta t = 0$, we further study the dependence of polarization state modulation on the pump intensity (Figure 6j–o). When I_p increases from 0 (static) to 0.35 GW cm^{-2} , the polarization ellipse corresponding to the 1530 nm wavelength experiences an ellipticity decrease from 0.51 to 0.19 (upper panel of Figure 6k), while that corresponding to a 1540 nm wavelength shows an orientation rotation up to $\sim 40^\circ$ (lower panel of Figure 6m). For all three wavelengths that were studied, an approximately linear relationship between both η and $\Delta\theta$ and I_p was seen with no obvious saturation. We emphasize that the maximal pump intensity used in this measurement was roughly 2 orders of magnitude lower than that used in ref 45, which has demonstrated similarly strong polarization manipulation in the transmission mode.

In conclusion, we have demonstrated a nonlinear chiral meta-mirror for ultrafast all-optical switching of near-infrared light polarization. Our results show that the interference-enhanced Mie resonance in high-index nanophotonic structures leads to a strong enhancement of the light–matter interaction at the nanometer scale, offering a transformative approach to achieving photonic meta-devices for an extraordinarily strong chiroptical response and ultrafast polarization switching. The proposed hybrid chiral meta-mirrors show great promise, particularly for applications in polarization-sensitive all-optical information processing. Given the experimentally observed sharp chiral resonance and spin-selective near-field enhancement, we also envision that the proposed meta-mirrors can be used as chip-scale chiroptical platforms for highly sensitive enantiomeric sensing of biochemical substances.

■ ASSOCIATED CONTENT

SI Supporting Information

The Supporting Information is available free of charge at <https://pubs.acs.org/doi/10.1021/acs.nanolett.0c00007>.

Device fabrication, optical characterization, numerical simulations, and an additional discussion of the optical anisotropy and performance improvement of the meta-mirror (PDF)

■ AUTHOR INFORMATION

Corresponding Authors

Lei Kang – Department of Electrical Engineering, The Pennsylvania State University, University Park, Pennsylvania 16802, United States; orcid.org/0000-0001-7718-7756; Email: lzk12@psu.edu

Xingjie Ni – Department of Electrical Engineering, The Pennsylvania State University, University Park, Pennsylvania 16802, United States; Email: xingjie@psu.edu

Zhiwen Liu – Department of Electrical Engineering, The Pennsylvania State University, University Park, Pennsylvania 16802, United States; Email: zzl1@psu.edu

Douglas H. Werner – Department of Electrical Engineering, The Pennsylvania State University, University Park, Pennsylvania 16802, United States; Email: dhw@psu.edu

Authors

Cheng-Yu Wang – Department of Electrical Engineering, The Pennsylvania State University, University Park, Pennsylvania 16802, United States

Xuexue Guo – Department of Electrical Engineering, The Pennsylvania State University, University Park, Pennsylvania 16802, United States

Complete contact information is available at: <https://pubs.acs.org/doi/10.1021/acs.nanolett.0c00007>

Author Contributions

[†]L.K., C.-Y.W., and X.G. contributed equally.

Notes

The authors declare no competing financial interest.

■ ACKNOWLEDGMENTS

This work was partially funded by the Penn State MRSEC, Center for Nanoscale Science (NSF DMR-1420620), and by the DARPA EXTREME program (HR00111720032).

■ REFERENCES

- (1) Soukoulis, C. M.; Wegener, M. Past Achievements and Future Challenges in the Development of Three-Dimensional Photonic Metamaterials. *Nat. Photonics* **2011**, *5*, 523–530.
- (2) Liu, Y.; Zhang, X. Metamaterials: A New Frontier of Science and Technology. *Chem. Soc. Rev.* **2011**, *40*, 2494.
- (3) Zheludev, N. I.; Kivshar, Y. S. From Metamaterials to Metadevices. *Nat. Mater.* **2012**, *11*, 917–924.
- (4) Wang, Z.; Cheng, F.; Winsor, T.; Liu, Y. Optical Chiral Metamaterials: A Review of the Fundamentals, Fabrication Methods and Applications. *Nanotechnology* **2016**, *27*, 412001.
- (5) Qiu, M.; Zhang, L.; Tang, Z.; Jin, W.; Qiu, C.-W.; Lei, D. Y. 3D Metaphotonic Nanostructures with Intrinsic Chirality. *Adv. Funct. Mater.* **2018**, *28*, 1803147.
- (6) Gansel, J. K.; Thiel, M.; Rill, M. S.; Decker, M.; Bade, K.; Saile, V.; von Freymann, G.; Linden, S.; Wegener, M. Gold Helix Photonic Metamaterial as Broadband Circular Polarizer. *Science* **2009**, *325*, 1513.
- (7) Gao, W.; Leung, H. M.; Li, Y.; Chen, H.; Tam, W. Y. Circular Dichroism in Double-Layer Metallic Crossed-Gratings. *J. Opt.* **2011**, *13*, 115101.
- (8) Zhao, Y.; Belkin, M. A.; Alù, A. Twisted Optical Metamaterials for Planarized Ultrathin Broadband Circular Polarizers. *Nat. Commun.* **2012**, *3*, 870.
- (9) Yin, X.; Schäferling, M.; Metzger, B.; Giessen, H. Interpreting Chiral Nanophotonic Spectra: The Plasmonic Born–Kuhn Model. *Nano Lett.* **2013**, *13*, 6238–6243.
- (10) Cui, Y.; Kang, L.; Lan, S.; Rodrigues, S.; Cai, W. Giant Chiral Optical Response from a Twisted-Arc Metamaterial. *Nano Lett.* **2014**, *14*, 1021–1025.
- (11) Kang, L.; Lan, S.; Cui, Y.; Rodrigues, S. P.; Liu, Y.; Werner, D. H.; Cai, W. An Active Metamaterial Platform for Chiral Responsive Optoelectronics. *Adv. Mater.* **2015**, *27*, 4377–4383.
- (12) Zhang, C.; Pfeiffer, C.; Jang, T.; Ray, V.; Junda, M.; Upreti, P.; Podraza, N.; Grbic, A.; Guo, L. J. Breaking Malus' Law: Highly Efficient, Broadband, and Angular Robust Asymmetric Light Transmitting Metasurface. *Laser Photonics Rev.* **2016**, *10*, 791–798.
- (13) Yin, X.; Schäferling, M.; Michel, A.-K. U.; Tittel, A.; Wuttig, M.; Taubner, T.; Giessen, H. Active Chiral Plasmonics. *Nano Lett.* **2015**, *15*, 4255–4260.
- (14) Yu, N.; Genevet, P.; Kats, M. A.; Aieta, F.; Tetienne, J.-P.; Capasso, F.; Gaburro, Z. Light Propagation with Phase Discontinuities: Generalized Laws of Reflection and Refraction. *Science* **2011**, *334*, 333–337.

- (15) Ni, X.; Emani, N. K.; Kildishev, A. V.; Boltasseva, A.; Shalae, V. M. Broadband Light Bending with Plasmonic Nanoantennas. *Science* **2012**, *335*, 427–427.
- (16) Yin, X.; Ye, Z.; Rho, J.; Wang, Y.; Zhang, X. Photonic Spin Hall Effect at Metasurfaces. *Science* **2013**, *339*, 1405–1407.
- (17) Ni, X.; Wong, Z. J.; Mrejen, M.; Wang, Y.; Zhang, X. An Ultrathin Invisibility Skin Cloak for Visible Light. *Science* **2015**, *349*, 1310–1314.
- (18) Yu, N.; Aieta, F.; Genevet, P.; Kats, M. A.; Gaburro, Z.; Capasso, F. A Broadband, Background-Free Quarter-Wave Plate Based on Plasmonic Metasurfaces. *Nano Lett.* **2012**, *12*, 6328–6333.
- (19) Devlin, R. C.; Ambrosio, A.; Rubin, N. A.; Mueller, J. P. B.; Capasso, F. Arbitrary Spin-to-Orbital Angular Momentum Conversion of Light. *Science* **2017**, *358*, 896–901.
- (20) Wu, C.; Arju, N.; Kelp, G.; Fan, J. A.; Dominguez, J.; Gonzales, E.; Tutuc, E.; Brener, I.; Shvets, G. Spectrally Selective Chiral Silicon Metasurfaces Based on Infrared Fano Resonances. *Nat. Commun.* **2014**, *5*, 3892.
- (21) Wang, Z.; Jia, H.; Yao, K.; Cai, W.; Chen, H.; Liu, Y. Circular Dichroism Metamirrors with Near-Perfect Extinction. *ACS Photonics* **2016**, *3*, 2096–2101.
- (22) Li, W.; Coppens, Z. J.; Besteiro, L. V.; Wang, W.; Govorov, A. O.; Valentine, J. Circularly Polarized Light Detection with Hot Electrons in Chiral Plasmonic Metamaterials. *Nat. Commun.* **2015**, *6*, 8379.
- (23) Kang, L.; Rodrigues, S. P.; Taghinejad, M.; Lan, S.; Lee, K.-T.; Liu, Y.; Werner, D. H.; Urbas, A.; Cai, W. Preserving Spin States upon Reflection: Linear and Nonlinear Responses of a Chiral Meta-Mirror. *Nano Lett.* **2017**, *17*, 7102–7109.
- (24) Kivshar, Y. All-Dielectric Meta-Optics and Non-Linear Nanophotonics. *Natl. Sci. Rev.* **2018**, *5*, 144–158.
- (25) Kruk, S.; Kivshar, Y. Functional Meta-Optics and Nanophotonics Governed by Mie Resonances. *ACS Photonics* **2017**, *4*, 2638–2649.
- (26) Liu, S.; Sinclair, M. B.; Mahony, T. S.; Jun, Y. C.; Campione, S.; Ginn, J.; Bender, D. A.; Wendt, J. R.; Ihlefeld, J. F.; Clem, P. G.; et al. Optical Magnetic Mirrors without Metals. *Optica* **2014**, *1*, 250–256.
- (27) Shcherbakov, M. R.; Neshev, D. N.; Hopkins, B.; Shorokhov, A. S.; Staude, I.; Melik-Gaykazyan, E. V.; Decker, M.; Ezhov, A. A.; Miroshnichenko, A. E.; Brener, I.; et al. Enhanced Third-Harmonic Generation in Silicon Nanoparticles Driven by Magnetic Response. *Nano Lett.* **2014**, *14*, 6488–6492.
- (28) Kruk, S. S.; Camacho-Morales, R.; Xu, L.; Rahmani, M.; Smirnova, D. A.; Wang, L.; Tan, H. H.; Jagadish, C.; Neshev, D. N.; Kivshar, Y. S. Nonlinear Optical Magnetism Revealed by Second-Harmonic Generation in Nanoantennas. *Nano Lett.* **2017**, *17*, 3914–3918.
- (29) Li, G.; Zhang, S.; Zentgraf, T. Nonlinear Photonic Metasurfaces. *Nat. Rev. Mater.* **2017**, *2*, 17010.
- (30) Kang, L.; Jenkins, R. P.; Werner, D. H. Recent Progress in Active Optical Metasurfaces. *Adv. Opt. Mater.* **2019**, *7*, 1801813.
- (31) Taghinejad, M.; Cai, W. All-Optical Control of Light in Micro- and Nanophotonics. *ACS Photonics* **2019**, *6*, 1082–1093.
- (32) Fu, Y. H.; Kuznetsov, A. I.; Miroshnichenko, A. E.; Yu, Y. F.; Luk'yanchuk, B. Directional Visible Light Scattering by Silicon Nanoparticles. *Nat. Commun.* **2013**, *4*, 1527.
- (33) Miroshnichenko, A. E.; Evlyukhin, A. B.; Yu, Y. F.; Bakker, R. M.; Chipouline, A.; Kuznetsov, A. I.; Luk'yanchuk, B.; Chichkov, B. N.; Kivshar, Y. S. Nonradiating Anapole Modes in Dielectric Nanoparticles. *Nat. Commun.* **2015**, *6*, 8069.
- (34) Rybin, M. V.; Koshelev, K. L.; Sadrieva, Z. F.; Samusev, K. B.; Bogdanov, A. A.; Limonov, M. F.; Kivshar, Y. S. High-Q Supercavity Modes in Subwavelength Dielectric Resonators. *Phys. Rev. Lett.* **2017**, *119*, 243901.
- (35) Chen, W. T.; Zhu, A. Y.; Sanjeev, V.; Khorasaninejad, M.; Shi, Z.; Lee, E.; Capasso, F. A Broadband Achromatic Metalens for Focusing and Imaging in the Visible. *Nat. Nanotechnol.* **2018**, *13*, 220–226.
- (36) Shcherbakov, M. R.; Vabishchevich, P. P.; Shorokhov, A. S.; Chong, K. E.; Choi, D.-Y.; Staude, I.; Miroshnichenko, A. E.; Neshev, D. N.; Fedyanin, A. A.; Kivshar, Y. S. Ultrafast All-Optical Switching with Magnetic Resonances in Nonlinear Dielectric Nanostructures. *Nano Lett.* **2015**, *15*, 6985–6990.
- (37) Sugimoto, H.; Fujii, M. Broadband Dielectric–Metal Hybrid Nanoantenna: Silicon Nanoparticle on a Mirror. *ACS Photonics* **2018**, *5*, 1986–1993.
- (38) Deng, F.; Liu, H.; Lan, S. Metal Substrate-Induced Line Width Compression in the Magnetic Dipole Resonance of a Silicon Nanosphere Illuminated by a Focused Azimuthally Polarized Beam. *Nanoscale Res. Lett.* **2018**, *13*, 395.
- (39) Kang, L.; Bao, H.; Werner, D. H. Interference-Enhanced Optical Magnetism in Surface High-Index Resonators: A Pathway toward High-Performance Ultracompact Linear and Nonlinear Meta-Optics. *Photonics Res.* **2019**, *7*, 1296–1305.
- (40) Piper, J. R.; Fan, S. Total Absorption in a Graphene Monolayer in the Optical Regime by Critical Coupling with a Photonic Crystal Guided Resonance. *ACS Photonics* **2014**, *1*, 347–353.
- (41) Plum, E.; Zheludev, N. I. Chiral Mirrors. *Appl. Phys. Lett.* **2015**, *106*, 221901.
- (42) Dani, K. M.; Ku, Z.; Upadhy, P. C.; Prasankumar, R. P.; Brueck, S. R. J.; Taylor, A. J. Subpicosecond Optical Switching with a Negative Index Metamaterial. *Nano Lett.* **2009**, *9*, 3565–3569.
- (43) Cho, D. J.; Wu, W.; Ponizovskaya, E.; Chaturvedi, P.; Bratkovsky, A. M.; Wang, S.-Y.; Zhang, X.; Wang, F.; Shen, Y. R. Ultrafast Modulation of Optical Metamaterials. *Opt. Express* **2009**, *17*, 17652–17657.
- (44) Yang, Y.; Kelley, K.; Sacht, E.; Campione, S.; Luk, T. S.; Maria, J.-P.; Sinclair, M. B.; Brener, I. Femtosecond Optical Polarization Switching Using a Cadmium Oxide-Based Perfect Absorber. *Nat. Photonics* **2017**, *11*, 390–395.
- (45) Nicholls, L. H.; Rodríguez-Fortuño, F. J.; Nasir, M. E.; Córdova-Castro, R. M.; Olivier, N.; Wurtz, G. A.; Zayats, A. V. Ultrafast Synthesis and Switching of Light Polarization in Nonlinear Anisotropic Metamaterials. *Nat. Photonics* **2017**, *11*, 628.
- (46) Taghinejad, M.; Taghinejad, H.; Xu, Z.; Lee, K.-T.; Rodrigues, S. P.; Yan, J.; Adibi, A.; Lian, T.; Cai, W. Ultrafast Control of Phase and Polarization of Light Expedited by Hot-Electron Transfer. *Nano Lett.* **2018**, *18*, 5544–5551.
- (47) Della Valle, G.; Hopkins, B.; Ganzer, L.; Stoll, T.; Rahmani, M.; Longhi, S.; Kivshar, Y. S.; De Angelis, C.; Neshev, D. N.; Cerullo, G. Nonlinear Anisotropic Dielectric Metasurfaces for Ultrafast Nanophotonics. *ACS Photonics* **2017**, *4*, 2129–2136.